A functional genome-wide genetic screening identifies new pathways controlling the G1/S transcriptional wave

Laura Gaspa*, Alberto González-Medina*, Elena Hidalgo and José Ayté

Oxidative Stress and Cell Cycle Group, Universitat Pompeu Fabra, Barcelona, Spain.

* The first two authors contributed equally to this work

Correspondence should be addressed to José Ayté (jose.ayte@upf.edu)

Keywords: G1/S transition; MBF complex; Cdc22-YFP; *S. pombe*; Elongator; COP9;

Running title: Isolation of new MBF regulators

22 **ABSTRACT**

23 The *Schizosaccharomyces pombe* MBF complex activates the transcription of genes
24 required for DNA synthesis and S phase. The MBF complex contains several proteins,
25 including the core components Cdc10, Res1 and Res2, the co-repressor proteins Yox1
26 and Nrm1 and the co-activator Rep2. It has recently been shown how MBF is regulated
27 when either the DNA damage or the DNA synthesis checkpoints are activated.
28 However, how MBF is regulated in a normal unperturbed cell cycle is still not well
29 understood. We have set up a genome-wide genomic screen searching for global
30 regulators of MBF. We have crossed our knock-out collection library with a reporter
31 strain that allows the measurement of MBF activity in live cells by flow cytometry. We
32 confirm previously known regulators of MBF and show that COP9/signalosome and
33 tRNA methyltransferases also regulate MBF activity.

INTRODUCTION

During its life cycle, fission yeast cells face with a critical decision between vegetative growth, sexual conjugation, or remaining in stationary phase. This decision point, known as Start in yeasts and restriction point in metazoans, occurs in late G1 phase of the cell cycle. Genetic analyses have identified several proteins that are required for passage through Start in fission yeast. Among them, we can find the cyclin-dependent kinase, Cdc2 [1] and the activity of the transcription factor MBF, which is a multimeric complex whose core proteins are Cdc10, Res1 and Res2. [2-4] MBF, which is the functional analog of mammalian pRB/E2F, drives the G1-to-S wave of transcription, controlling the expression of some genes that are directly or indirectly required for DNA synthesis, such as *cdc18* (the fission yeast homolog to CDC6), *cdt1* and the gene coding for ribonucleotide reductase, *cdc22*. [3, 5, 6]

We have shown that while *cig2* is one of the genes that is under the control of MBF, the protein encoded by this gene, the cyclin Cig2, is also part of a negative feed-back loop that phosphorylates and inhibits MBF. [7] Another level of regulation is achieved by the repressor system Nrm1/Yox1. It has been shown that Yox1 binds the MBF complex through the co-repressor Nrm1, mainly at the end of S phase and during G2, when MBF-dependent transcription is down-regulated. [8-11] However, when DNA replication is challenged (i.e., treatment with hydroxyurea), Yox1 is phosphorylated by the effector kinase of the DNA synthesis checkpoint, Cds1. Once phosphorylated, Yox1 is released from MBF and MBF-dependent transcription is activated until cells overcome the block to DNA replication. Cells harboring a Yox1 mutant (Yox1-SATA) that cannot be phosphorylated by Cds1 are unable to induce MBF-dependent transcription when DNA replication is challenged with hydroxyurea. Interestingly, Yox1-SATA cells are still able to induce MBF-dependent transcription during S phase of a normal unperturbed cell cycle, pointing to the fact that Yox1 phosphorylation has a role in the DNA replication checkpoint, but not during a normal unperturbed S phase. Contrary to this positive effect on MBF-dependent transcription by the DNA synthesis checkpoint, in response to DNA damage (i.e. γ-irradiation, MMS treatment, etc) the outcome has been shown to be the opposite: MBF-dependent transcription is inhibited. This is achieved by direct phosphorylation of two specific residues located at the carboxy-terminal domain of Cdc10 by the effector kinase of the DNA-damage checkpoint, Chk1. [12] This phosphorylation induces the release of MBF from its target

67 promoters, repressing MBF-dependent transcription. When these residues in Cdc10 are
68 mutated to non-phosphorylatable amino acids, fission yeast cells are highly sensitive to
69 DNA damaging agents. Thus, Yox1 and Cdc10 couple normal cell cycle regulation and
70 the DNA-synthesis and DNA-damage checkpoints in a single transcriptional complex.

71 Like its mammalian counterpart, the regulated activity of the MBF complex is
72 essential for the normal G1-to-S transition: cells with hypoactive MBF complex are
73 unable to complete S phase while cells with hyperactive MBF show genomic instability.
74 [8] Thus, tight and precise regulation of the MBF complex activity is essential to avoid
75 major problems, no matter whether in a unicellular cell or in a pluricellular organism.
76 In this work, we describe a genome-wide genetic screening to identify all non-essential
77 fission yeast proteins required for regulation of the MBF complex activity. This
78 screening identified known regulators of MBF activity (like Res1, Res2, Yox1, Nrm1
79 and Rep2), but also some proteins of the COP9/signalosome and several tRNA
80 methyltransferases.

81 **RESULTS**

82 **Cdc22-YFP as a reporter strain to measure MBF activity *in vivo***

83 We wanted to carry out a genome-wide screening of *S. pombe* to identify potential MBF
84 regulators. The first step was to select an appropriate reporter with enough sensitivity to
85 allow measurement of its activity directly on cells in culture, but also with good
86 reproducibility between different biological replicates or conditions. We generated
87 different strains that either were expressing chimeras of a fluorescent protein (YFP or
88 GFP) fused to MBF-regulated genes (Cdc22-YFP, Yox1-GFP or Tos4-GFP) or were
89 expressing YFP directly under the control of MBF-regulated promoters (p*cdc18*, p*cdt2*,
90 p*mik1* or p*tos4*). [3, 11, 13, 14] By microscopic observation, we could detect fluorescence in
91 each of the seven strains that we tested, but with different intensity. Since we wanted to
92 establish a method that would allow quantifying this fluorescence, we decided to
93 determine their intrinsic fluorescence on the cytometer. As shown in Fig. 1A, only the
94 strain expressing Cdc22-YFP in its own locus showed differential fluorescence (10-fold
95 increase fluorescence) when compared with the parental wild type strain (compare WT
96 with Cdc22-YFP bars). Next, since we also needed a control reporter to measure
97 constitutive transcription, we placed a cassette containing mRFP under the control of
98 housekeeping promoters with constitutive cell cycle transcription, such as *srp2*, *act1* or
99 *sty1* (Fig. 1B). Red fluorescence was detected in all three strains and quite proportional
100 to the strength of the promoter, with *sty1* promoter being the strongest one.

101 As a proof-of-concept that the Cdc22-YFP reporter could measure changes in
102 MBF activity, we integrated both reporters (Cdc22-YFP and p*sty1*-RFP) in the same
103 strain. Then we deleted known regulators of MBF activity (the repressor Yox1 or the
104 co-activator Rep2) or non-essential elements of the MBF complex (Res1 or Res2). As
105 expected, deletion of the repressor Yox1 increased the yellow fluorescence of the cells
106 without affecting the red fluorescence; on the contrary, deleting *rep2* decreased the
107 yellow fluorescence (Fig. 1C). Next, we wanted to determine if the reporter strain could
108 measure the changes in a quantitative manner that mirrors the changes in the
109 transcription of MBF-dependent genes. To do so, we measured red and yellow
110 fluorescence of the different strains on the cytometer. As shown in Fig. 1D, either the
111 yellow fluorescence values alone (YFP, on the FITC channel) or the ratios to the red
112 fluorescence (YFP/RFP) or to the size (YFP/FSC) showed similar values, with the later

113 one displaying higher reproducibility and consequently lower standard variations.
114 Interestingly, the steady-state levels of Cdc22-YFP [measured on quantitative Western
115 blot (WB)] and the mRNA levels (measured by Q-PCR) showed similar increases or
116 decreases to the fluorescence measured on FACS (Fig. 1D). This confirmed that our
117 reporter strain (Cdc22-YFP p*sty1*-RFP) satisfactorily reflects the endogenous MBF
118 activity.

119 **Genome-wide screening to isolate genes that regulate MBF activity**

120 To confirm that the Cdc22-YFP reporter could be used in a genome-wide screen to
121 identify MBF regulators, we crossed the reporter strain with the laboratory knock-out
122 collection of chromatin modifiers, including the histone acetylases (HATs) *Δhat1*,
123 *Δgcn5* and *Δrtt109*, the histone deacetylases (HDACs) *Δhos2*, *Δsir2*, *Δhst2*, *Δhst4* and
124 *Δclr3*, the histone methyltransferases *Δset1* and *Δset2*, and several other general
125 chromatin remodelers (Figs. 2A-B). To test the reproducibility of the process when the
126 strains were grown in 96-well plates, we analyzed the above chromatin-modifier strain
127 mutants and compared the results obtained from cultures grown in individual test tubes
128 to the results obtained from cultures of the same strains grown in 96-well plates. As
129 shown in Fig. 2B, there are minor differences in the read-out, independent of how the
130 different strains were processed, either in tubes/flasks or in 96-well plates. Among the
131 twenty strains that we tested, we only detected a clear effect on the YFP/FSC or
132 YFP/RFP in *Δnrm1*, *Δyox1* (both not shown in the plot), *Δrep2*, *Δres1*, *Δres2* and *Δhst4*.
133 We were expecting to observe changes in the fluorescence read-out from the MBF
134 mutants (the first five strains); we could also detect a significant increase in the strain
135 lacking Hst4, an HDAC from the sirtuin family,[15, 16] suggesting that this HDAC could
136 be involved in the repression of MBF-dependent transcription. However, it should be
137 noted that the other sirtuins (Sir2 and Hst2) had no effect in the YFP/FSC or YFP/RFP
138 ratios.

139 Next, we crossed in the reporter strain with the haploid gene deletion collection
140 from Bioneer, containing 3005 different strains. [17] High throughput crossing of the
141 reporter strain with the deletion library in 96-well plates followed by direct plating on
142 selective media allowed the isolation of haploid strains, each one with a single gene
143 deletion and the Cdc22-YFP and the p*sty1*-RFP reporters. Of the total collection, we
144 were able to cross and measure a YFP/FSC ratio in 2792 strains, which represents

145 92.9% of the original strain collection. At least two different biological replicates of
146 each strain were processed and analyzed through the cytometer. Since all the 96-well
147 plates were grown and processed through the cytometer on different days and the laser
148 of the cytometer has a considerable variation in its level of sensitivity from day to day,
149 we decided to include a *Δyox1*, a *Δrep2* and a wild type strain in each plate. These
150 strains were used as quality control after normalization of each plate. Then, the YFP
151 (FITC) value of each of the 2792 strains was plotted against the FSC value (Fig. 2C).
152 We selected the top and the bottom 1st percentile of the YFP/FSC ratio and plotted the
153 corresponding strains marked as red dots in Fig. 2C. This representation was selected
154 since it helped to discriminate strains with high fluorescence values caused because they
155 were large cells and consequently accumulated more YFP (and not because they had a
156 strong induction of MBF activity); or the opposite: cells with low fluorescence values
157 because they were small (see grey dot with low FITC values in the bottom left quadrant
158 of Fig. 2C). Thus, for each strain we can discriminate the contribution to the YFP/FSC
159 value of both, transcriptional levels (YFP value) and cell size (FSC value). Taking into
160 consideration the values of the 2792 analyzed strains, we obtained a mean YFP/FSC
161 value of 1.00, with a standard deviation of ±0.21. Thus, we decided to focus on the top
162 and bottom 1st percentile with values that were over 2-fold SD (over 1.55 or below
163 0.60), reducing the putative hits to 17 different strains with lower MBF activity (Table
164 1) and 32 strains with higher MBF activity (Table 2). It caught our attention that among
165 the 17 strains with lower YFP/FSC ratios, there was an enrichment of strains in which
166 translation efficiency could be hampered (including mutants of Elongator, ribosomal
167 proteins and tRNA modification pathway). In contrast, among the group of strains with
168 higher YFP/FSC ratios, there was an apparent enrichment of cell cycle mutants. To
169 know exactly if there was such bias to different types of mutants, we extended the list of
170 genes in both categories to the bottom 140 and the top 139 (which represent the 5th
171 percentile; green dots in Fig. 2C) and used Gene Ontology (GO) system to assign genes
172 to a specific biological process. This revealed that among the strains with low
173 YFP/FSC ratio there was a clear enrichment of genes involved in Translation, Ribosome
174 biogenesis, tRNA processing and Protein assembly (Fig. 2D), while among the strains
175 with high YFP/FSC ratio there was an enrichment for the terms of Cytokinesis, Cell
176 cycle regulation, DNA replication and DNA repair (Fig. 2E).

tRNA methylation and Elongator mutants have impaired MBF-dependent transcription

Given the previous observation indicating that several mutants of the tRNA methylation pathway had low YFP/FSC ratio, we decided to investigate if this pathway was indeed affecting MBF-dependent transcription. As shown in Fig. 3A, several mutant strains in the pathway involved in tRNA methylation had low YFP/FSC values (marked as red dots in the plot). To confirm this possibility we prepared RNA from asynchronous cultures of wild type (WT) cells, *Δyox1* and *Δrep2* and from several mutants of the tRNA methylation pathway. As shown in Fig. 3B, there was an overall decrease in the level of MBF-dependent transcription in *Δtrm112*, *Δmtq2* and *Δtrm9* cells, measured as the amount of *cdc18* mRNA. This effect was not so clear in the other mutants that we tested (*Δtrm11*, *Δlys9* and *Δbud23*). This fact was not completely surprising, since Trm112 dimerizes with another protein (either Trm9 or Mtq2) to form an active methylase that modifies specific nucleotides in tRNAs. [19] However, and despite these strains displaying decreased MBF activity (measured with the reporter strain or as the level of *cdc18* transcript), none of these mutants were sensitive to hydroxyurea (HU) (Fig. 3C). One possible hypothesis that could explain the impaired MBF-dependent transcription in the tRNA methylation mutants could be that a specific activator of MBF activity (i.e. Rep2) could have impaired translation efficiency. In fact, in a genome-wide analysis it was recently proposed that Rep2 could present low levels of translation efficiency in some mutants of the pathway (27% to 31%, compared to a wild type strain). [18] We decided to test whether in a *Δtrm112* strain there was a limited amount of Rep2. As shown in Fig. 3D, we could not observe any difference in the amount of Rep2 between a wild type and a *Δtrm112* strain.

Related to the tRNA modifying enzymes, Elongator complex also promotes efficient translation. We recently reported that the activity of this complex was required for proper tolerance to H_2O_2 stress and that this effect was mediated by enhanced translation of the transcription factor Atf1. [19] From the 6 subunits of the Elongator complex, only *Δelp2* and *Δelp5* had wild type YFP/FSC ratios, with *Δiki3*/*Δelp1* and *Δelp4* having the lowest YFP/FSC ratios (0.52) of all the strains that we tested from the knock-out collection, even below the strain lacking the known MBF co-activator Rep2 (0.55) (Fig. 3E and Table 1). To confirm that the effect measured with the reporter strain was on MBF-dependent transcription, we isolated RNA from wild type, *Δyox1*

210 and *Δrep2* cells as well as from *Δiki3*/*Δelp1* and *Δctu1* cells. We used *Δctu1* cells since
211 the Ctu1-Ctu2 complex catalyzes the thiolation at carbon 2 of U_{34} (s^2U_{34}) [20] and the
212 modification of specific tRNAs is sequentially made by Trm112 complex and the Ctu1-
213 Ctu2 complex. In fact, although *Δctu1* is not included in Table 1 containing the lowest
214 YFP/FSC strains from our screening, *Δctu1* strain had also a low YFP/FSC ratio (0.66).
215 As shown in Fig. 3F, we observed a clear reduction of MBF-dependent transcription in
216 *Δiki3*/*Δelp1* cells, similar to the level observed in *Δrep2* cells.

217 **COP9/signalosome mutants have induced MBF activity**

218 Among the mutants with higher YFP/FSC ratio we found *Δnrm1* and *Δyox1* with the
219 highest ratio (5.39 and 4.91, respectively), as expected. We observed that several
220 mutants of COP9/signalosome had a high YFP/FSC ratio, including *Δcsn1* and *Δcsn2*.
221 Interestingly, we also detected increased YFP/FSC ratios in mutants of the COP9-
222 regulated E3 ubiquitin ligase complex Cul4-Ddb1^{Cdt2}, *Δcdt2* and *Δddb1* (Table 2 and
223 Fig. 4A). To confirm that the effect was directly on MBF activity, we prepared RNA
224 from asynchronous cultures of wild type cells, *Δyox1 and Δrep2* (as positive and
225 negative regulators of MBF activity) and from several mutants of the COP/signalosome
226 pathway. As shown in Fig. 4B, there was an overall increase in the level of MBF-
227 dependent transcription, which was more noticeable in *Δddb1* and *Δcdt2* cells, measured
228 as the amount of *cdc18* mRNA.

229 The Cul4-Ddb1^{Cdt2} complex is implicated in the regulation of at least two
230 substrate proteins: Spd1, an inhibitor of ribonucleotide reductase, and Epe1, a
231 heterochromatin regulator. [21] Spd1 and Epe1 accumulate in cells lacking Ddb1, Cdt2 or
232 with defective COP9, inducing defects in cell cycle and in heterochromatin silencing.
233 Since the defects in cell cycle are largely rescued by deletion of the ribonucleotide
234 reductase inhibitor, Spd1,[22, 23] we hypothesized that these strains could have an
235 increased basal activation of the DNA-synthesis checkpoint. One of the consequences
236 of activating Cds1, the effector kinase of this checkpoint, is the phosphorylation of
237 Yox1. [11] Yox1 phosphorylation by Cds1 induces its release from MBF and the
238 activation of MBF-dependent transcription, which in turn allows overcoming the arrest
239 imposed by the nucleotide depletion. To test this possibility we determined the status of
240 Yox1 phosphorylation in these mutants. As shown in Fig. 4C, Yox1 is phosphorylated
241 in *Δcsn1*, *Δcsn2*, *Δcdt2* and *Δddb1* strains, and to similar level as in a wild type strain

242 treated with hydroxyurea (WT + HU). Furthermore, this phosphorylation is abolished
243 when Spd1 is deleted (in a *Δddb1* or in a *Δcdt2* background), indicating that in these
244 genetic backgrounds the checkpoint is not activated in basal conditions.

245 Despite COP9 or E3 ubiquitin ligase complex Cul4-Ddb1^{Cdt2} mutants have
246 increased MBF activity (measured with the reporter strain or as the level of *cdc18*
247 transcript), all these mutants were still highly sensitive to HU (Fig. 4D). We also tested
248 the double mutants (*Δddb1Δspd1* and *Δcdt2Δspd1*) in our spot assay, but were unable to
249 increase the resistance to HU treatment (Fig. 4D). In spite of this observation, the
250 genetic interaction between E3 ubiquitin ligase complex Cul4-Ddb1^{Cdt2} mutants and the
251 DNA synthesis checkpoint was clearly confirmed by tetrad dissection. As shown in
252 Figs. 4E,F, double mutants *Δddb1Δrad3* and *Δddb1Δcds1* are not viable, pointing that
253 the checkpoint needs to be activated in a *Δddb1* background or the cells cannot survive
254 to the depletion of nucleotides.

DISCUSSION

The MBF complex is an essential transcription factor that in *S. pombe* cells controls the expression of the G1-to-S transcription program. Like its metazoan functional analog (pRB/E2F), the regulated activity of this complex is essential for the normal G1/S transition: cells with hypoactive MBF complex are unable to complete S phase while cells with hyperactive MBF show genomic instability. [8, 24] When DNA replication is challenged (i.e. after treating cells with HU), fission yeast cells activate their effector kinase (Cds1) and, among many other effects, are able to maintain a high level of MBF-dependent transcription. [11] To better understand how MBF is activated at the onset of each cell cycle, we have carried out a screening aiming to isolate non-essential genes that regulate MBF activity. The first step was the selection of a reporter system that would mirror MBF activity with high fidelity. Among all the reporter systems that we have assayed, fusing YFP to the carboxy-terminus of Cdc22 was the one that rendered most consistent and reproducible data. Similarly, we also needed a control and we used RFP driven by the promoter of *sty1*, which is a gene that has high level of transcription that is not cell cycle regulated. In parallel, we also used the size of the cells (FSC in the cytometer), which allows compensating for the accumulation of YFP in large cells (which otherways would be interpreted as high level of MBF activation).

We managed to cross 2792 different strains in 96-well plates and screen them in an automated cytometer. The screening has rendered 32 mutants with high YFP/FSC ratio and 17 with low ratio. We note that this screening was done measuring steady-state levels of the chimera Cdc22-YFP in asynchronous cultures of fission yeast. This has some limitations, since we are using a protein activity (YFP fluorescence) to measure transcription activity. Also, the fact that both Cdc22 and YFP are long-lived proteins brings an extra layer of difficulty measuring rapid transcriptional changes (especially those that decrease transcription). The use of more dynamic reporters (for example a short-lived Cdc22-YFP) would allow improving the measurement of small or transient changes in MBF activity, especially when MBF is down-regulated. Despite this, we have proved that in the reporter strain that we have used there is an excellent correlation between changes in MBF-dependent transcription and the fluorescence of the Cdc22-YFP strain (Fig. 1D).

286 In our screening, we isolated several mutants of the tRNA methylation pathway
287 and from the Elongator complex, which are involved in efficient translation of some
288 mRNAs. Interestingly, we also isolated several ribosomal proteins (Rps and Rpl strains
289 in Table 1), which points in the same direction: efficient translation is required for
290 activation of the MBF complex. In fact, Rep2 is one of the proteins that is supposed to
291 be not well translated in some Elongator mutants. [20] However, we do not observe any
292 decrease in the amount of Rep2 that is present in cells of Elongator or tRNA
293 methylation mutants (Fig. 3D). Further work will be required to determine how
294 translation efficiency may have an impact on the G1-to-S transcriptional wave.

295 Finally, we have found that deletions of two of the components of the fission
296 yeast COP9/signalosome (Csn1 and Csn2) and also deletions of non-essential
297 components of the COP9-regulated E3 ubiquitin ligase complex Cul4-Ddb1^{Cdt2}, induce
298 MBF-dependent transcription. Although we cannot rule out other mechanisms, it seems
299 that the major impact on MBF regulation is done through the stabilization of the
300 ribonucleotide reductase inhibitor Spd1, which in turn causes, sequentially, the
301 activation of the DNA synthesis checkpoint, phosphorylation of Yox1 and activation of
302 MBF-dependent transcription. Whether COP9 and the E3 ubiquitin ligase complex
303 Cul4-Ddb1^{Cdt2} impacts on MBF regulation through other mechanisms, still has to be
304 determined.

305 ## MATERIALS AND METHODS

306 ### Strains and media

307 All *S. pombe* strains used in this study are listed in Table 3. Media were prepared as
308 previously described. [25]

309 ### Construction of the reporter strain

310 Reporter strain JA1845 was generated by crossing JA1818 with P392. [26, 27] Double-
311 tagged, cycloheximide sensitive and h- meiotic products were selected and crossed to
312 the wild type strain to assess inheritance of *rpl42::cyh*^{R}. Only parental strains with
313 cycloheximide resistant descendents were selected as reporter strain.

314 ### Generation of the reporter library by systematic crossing

315 PEM2 (Pombe Epistatic Mapping) approach [26] was used to systematically cross the
316 Bioneer *S. pombe* Gene Deletion Library, arrayed in 96-well plates, with the reporter
317 strain JA1845. Plates from the library and a plate containing the JA1845 strain were
318 thawed and spotted into single-well plates containing YE5S + G418 and YE5S +
319 Hygromycin agar, respectively. After growing 2 days at 30ºC both plates were crossed
320 in MM-N solid agar using a 96-pin replicator and manual mixing. Mating plates were
321 kept at 25ºC for 4 days for sporulation. To eliminate diploid and haploid parental cells,
322 a replica in YE5S + Cycloheximide + G418 was performed and spores were allowed to
323 germinate 2 days at 30ºC. Finally, a last round of selection was applied using YE5S +
324 Cycloheximide + G418 + Hygromycin.

325 ### Sensitivity analysis

326 Cells were grown in liquid YE5S media to an OD600 of 0.3. Cultures were 10-fold
327 serially diluted in YE5S and spotted onto drug-free, 5 mM HU or 0,001% MMS
328 containing YE5S plates. Plates were incubated at 30ºC for 2-5 days.

329 ### RNA analysis

330 Total RNA from *S. pombe* rich medium cultures was obtained, processed and
331 transferred to membranes as described previously. [11] Membranes were hybridized with
332 the [α-^{32}P]dCTP-labeled *cdc18* and *act1* probes, containing the complete ORFs.

S. pombe TCA extracts and Western Blot analysis

Modified trichloroacetic acid (TCA) extracts were prepared as previously described. [28] Yox1-13Myc was immunodetected with polyclonal anti-Myc antibody (Sigma).

Flow cytometry

Sample preparation: Strains were inoculated in a 96-well plate with 200µl/well of YE5S+G418 using a 96 pin replicator (V&P Scientific). In each plate, rpd3-13Myc, Δyox1 and Δrep2, previously crossed with JA1845, were added with a pipette tip in empty wells H2, H3 and H12, as controls. Cultures were allowed to saturate by growing at 30ºC during 24h with no agitation. An approximate 1/50 dilution was then performed by pinning the saturated cultures into a U-shaped 96-well plate with 150µl/well of liquid YE5S. Plates were sealed with an impermeable membrane (Thermo Scientific) and kept at 30ºC O/N with agitation (1000rpm) to prevent sedimentation. Previous to flow cytometry acquisition, cultures were diluted with a 96 thick pin replicator to obtain a final concentration of approximately OD_{600} 0.025 ($0.5x10^6$ cells/sec).

Acquisition: BD FACSCanto™ flow cytometer with a BD High Throughput Sampler (HTS) was used for YFP quantification. YFP was excited at 488nm and detected using a 530/30 band-pass and 502 LP emission filter. Population of interest was obtained by hierarchical gating using i) forward (FSC) and side (SSC) light scattering ii) FSC-A against FSC-H to exclude debris and cell clumps iii) FITC-A and PerCP-Cy5-5-A. For each well, 85ul of sample were mixed 5 times at 90ul/s. 60ul were then analyzed at 2ul/sec and washed with 800ul of FACS Flow. 10.000 events were recorded for each well at ~$1x10^6$ events/sec. Data acquisition and processing was performed with BD FACSDiva Software 6.0.

Data processing: YFP/FSC (FITC/FSC) ratios for each well were calculated using raw FSC and FITC median values of the final gated population. To avoid plate-to-plate variation, FITC/FSC ratios of each well were normalized to the mean FITC/FSC ratio of the corresponding plate. 700 events were considered as the minimum threshold of counted events for trustable results. Each plate was analyzed in two separate replicas, and the mean of the duplicates was applied for each well to obtain the final FSC, FITC, and FITC/FSC normalized values. 99th percentile was calculated to define a list of “High ratio” and “Low ratio” hits, which included 32 and 17 genes respectively (with

364 values over 1.55 or below 0.60). We also calculated the 99th percentile to produce an
365 extended list of "High ratio" and "Low ratio" hits, which included 139 and 140 genes
366 respectively, which was used for the Gene ontology assignment.

367 **Gene ontology**

368 GO Slimmer was performed with AmiGO 1.8 using the GO Slim Terms list provided by
369 PomBase. Input lists were filtered using PomBase as database filter to reduce possible
370 ambiguity by excluding gene products not found in the database. All Evidence Codes
371 were applied, including IEA (Inferred from Electronic Annotation). For "All genes",
372 "High ratio", and "Low ratio", 592/2792, 14/139 and 12/140 genes were respectively
373 excluded for GO Slimmer calculation. To obtain fold enrichment values of each GO
374 Slim Term for "High ratio" and "Low ratio" lists, background correction was applied by
375 normalization with GO Slimmer results of all genes included in the screening.

ACKOWLEDGEMENTS

We are very thankful to Nevan Krogan for providing strain P392, Rafael Carazo-Salas for insightful comments on the screening and Oscar Fornas and staff from the Cytometry Facility at UPF for their help and support. We also thank members of the Oxidative Stress and Cell Cycle Group for help, suggestions and comments. We acknowledge the technical support of Mercè Carmona. This work was supported by grants from the Spanish Ministerio de Economia y Competitividad (BFU2012-31939), PLAN E and Feder. E. H. is recipient of an ICREA Academia Award (Generalitat de Catalunya, Spain).

385 **REFERENCES**

386 1. Nurse P, Bissett Y. Gene required in G1 for commitment to cell cycle and in G2 for control of mitosis
387 in fission yeast. Nature 1981; 292:558-60.

388 2. Caligiuri M, Beach D. Sct1 functions in partnership with Cdc10 in a transcription complex that
389 activates cell cycle START and inhibits differentiation. Cell 1993; 72:607-19.

390 3. Lowndes NF, McInerny CJ, Johnson AL, Fantes PA, Johnston LH. Control of DNA synthesis genes
391 in fission yeast by the cell-cycle gene cdc10+. Nature 1992; 355:449-53.

392 4. Zhu Y, Takeda T, Nasmyth K, Jones N. pct1+, which encodes a new DNA-binding partner of
393 p85cdc10, is required for meiosis in the fission yeast Schizosaccharomyces pombe. Genes Dev 1994;
394 8:885-98.

395 5. Rustici G, Mata J, Kivinen K, Lio P, Penkett CJ, Burns G, Hayles J, Brazma A, Nurse P, Bahler J.
396 Periodic gene expression program of the fission yeast cell cycle. Nat Genet 2004; 36:809-17.

397 6. Peng X, Karuturi RK, Miller LD, Lin K, Jia Y, Kondu P, Wang L, Wong LS, Liu ET,
398 Balasubramanian MK, et al. Identification of cell cycle-regulated genes in fission yeast. Mol Biol Cell
399 2005; 16:1026-42.

400 7. Ayté J, Schweitzer C, Zarzov P, Nurse P, DeCaprio JA. Feedback regulation of the MBF transcription
401 factor by cyclin Cig2. Nat Cell Biol 2001; 3:1043-50.

402 8. Caetano C, Limbo O, Farmer S, Klier S, Dovey C, Russell P, de Bruin RA. Tolerance of deregulated
403 G1/S transcription depends on critical G1/S regulon genes to prevent catastrophic genome instability. Cell
404 Rep 2014; 9:2279-89.

405 9. Ivanova T, Gomez-Escoda B, Hidalgo E, Ayte J. G1/S transcription and the DNA synthesis
406 checkpoint: common regulatory mechanisms. Cell Cycle 2011; 10:912-5.

407 10. Purtill FS, Whitehall SK, Williams ES, McInerny CJ, Sharrocks AD, Morgan BA. A homeodomain
408 transcription factor regulates the DNA replication checkpoint in yeast. Cell Cycle 2011; 10:664-70.

409 11. Gómez-Escoda B, Ivanova T, Calvo IA, Alves-Rodrigues I, Hidalgo E, Ayté J. Yox1 links MBF-
410 dependent transcription to completion of DNA synthesis. EMBO Rep 2011; 12:84-9.

411 12. Ivanova T, Alves-Rodrigues I, Gomez-Escoda B, Dutta C, DeCaprio JA, Rhind N, Hidalgo E, Ayte J.
412 The DNA damage and the DNA replication checkpoints converge at the MBF transcription factor. Mol
413 Biol Cell 2013; 24:3350-7.

414 13. Kiang L, Heichinger C, Watt S, Bahler J, Nurse P. Cyclin-dependent kinase inhibits reinitiation of a
415 normal S-phase program during G2 in fission yeast. Mol Cell Biol 2009; 29:4025-32.

416 14. Dutta C, Patel PK, Rosebrock A, Oliva A, Leatherwood J, Rhind N. The DNA replication checkpoint
417 directly regulates MBF-dependent G1/S transcription. Mol Cell Biol 2008; 28:5977-85.

418 15. Haldar D, Kamakaka RT. Schizosaccharomyces pombe Hst4 functions in DNA damage response by
419 regulating histone H3 K56 acetylation. Eukaryot Cell 2008; 7:800-13.

16. Freeman-Cook LL, Sherman JM, Brachmann CB, Allshire RC, Boeke JD, Pillus L. The Schizosaccharomyces pombe hst4(+) gene is a SIR2 homologue with silencing and centromeric functions. Mol Biol Cell 1999; 10:3171-86.

17. Kim DU, Hayles J, Kim D, Wood V, Park HO, Won M, Yoo HS, Duhig T, Nam M, Palmer G, et al. Analysis of a genome-wide set of gene deletions in the fission yeast Schizosaccharomyces pombe. Nat Biotech 2010; 28:617-23.

18. Bauer F, Matsuyama A, Candiracci J, Dieu M, Scheliga J, Wolf DA, Yoshida M, Hermand D. Translational control of cell division by Elongator. Cell Rep 2012; 1:424-33.

19. Fernandez-Vazquez J, Vargas-Perez I, Sanso M, Buhne K, Carmona M, Paulo E, Hermand D, Rodriguez-Gabriel M, Ayte J, Leidel S, et al. Modification of tRNA(Lys) UUU by elongator is essential for efficient translation of stress mRNAs. PLoS Genet 2013; 9:e1003647.

20. Dewez M, Bauer F, Dieu M, Raes M, Vandenhaute J, Hermand D. The conserved Wobble uridine tRNA thiolase Ctu1-Ctu2 is required to maintain genome integrity. Proc Natl Acad Sci U S A 2008; 105:5459-64.

21. Liu C, Powell KA, Mundt K, Wu L, Carr AM, Caspari T. Cop9/signalosome subunits and Pcu4 regulate ribonucleotide reductase by both checkpoint-dependent and -independent mechanisms. Genes Dev 2003; 17:1130-40.

22. Bayne EH, Bijos DA, White SA, de Lima Alves F, Rappsilber J, Allshire RC. A systematic genetic screen identifies new factors influencing centromeric heterochromatin integrity in fission yeast. Gen Biol 2014; 15:481.

23. Liu C, Poitelea M, Watson A, Yoshida SH, Shimoda C, Holmberg C, Nielsen O, Carr AM. Transactivation of Schizosaccharomyces pombe cdt2+ stimulates a Pcu4-Ddb1-CSN ubiquitin ligase. EMBO J 2005; 24:3940-51.

24. Ayte J, Leis JF, Herrera A, Tang E, Yang H, DeCaprio JA. The Schizosaccharomyces pombe MBF complex requires heterodimerization for entry into S phase. Mol Cell Biol 1995; 15:2589-99.

25. Moreno S, Klar A, Nurse P. Molecular genetic analysis of fission yeast Schizosaccharomyces pombe. Meth Enzymol 1991; 194:795-823.

26. Roguev A, Bandyopadhyay S, Zofall M, Zhang K, Fischer T, Collins SR, Qu H, Shales M, Park HO, Hayles J, et al. Conservation and rewiring of functional modules revealed by an epistasis map in fission yeast. Science 2008; 322:405-10.

27. Roguev A, Wiren M, Weissman JS, Krogan NJ. High-throughput genetic interaction mapping in the fission yeast Schizosaccharomyces pombe. Nature Meth 2007; 4:861-6.

28. Vivancos AP, Castillo EA, Biteau B, Nicot C, Ayte J, Toledano MB, Hidalgo E. A cysteine-sulfinic acid in peroxiredoxin regulates H2O2-sensing by the antioxidant Pap1 pathway. Proc Natl Acad Sci U S A 2005; 102:8875-80.

456 **FIGURE LEGENDS**

457 **Figure 1. Cdc22-YFP detects changes in MBF activity.** (**A**) Quantification of the
458 yellow fluorescence by FACS of the strains indicated on the right. Inset: raw data of the
459 wild type (WT) and reporter (Cdc22-YFP) strains. (**B**) Quantification of the red
460 fluorescence by flow cytometry of the strains indicated on the right. (**C**) Micrographs of
461 the strains indicated on the left. The reporter strain in a wild type background in
462 indicated (-). (**D**) Quantification of the parameters indicated in the inset in wild type
463 (WT), *Δyox1*, *Δrep2* and *Δres1* strains by FACS, quantitative Western Blot (WB) and
464 Q-PCR. Values were normalized to the wild type strain and plotted as mean ±SD of
465 biological triplicates.

466 **Figure 2. Genome-wide screening to identify regulators of MBF activity.** (**A**)
467 Cartoon representing the scheme followed to analyze the mini-library with the
468 chromatin modifiers mutants, either on 96-well plates or grown in individual tubes. (**B**)
469 Quantification of the YFP/FSC ratio of the strains indicated on the left bearing the
470 Cdc22-YFP reporter. For the 96-well plates, values are plotted as mean ±SD of
471 biological triplicates. (**C**) Plot of FITC (YFP fluorescence) vs FSC corresponding to the
472 2792 strains of the knock-out collection. Red dots correspond to the top and bottom 1st
473 percentile and green dots to the top and bottom 5th percentile of the FITC/FSC ratio.
474 The position of *Δyox1*, *Δnorm1* and *Δrep2* is indicated. (**D**) GO classification of the 140
475 strains with lower YFP/FSC ratio, represented as fold enrichment versus the whole
476 knock-out collection. (**E**) Same as (**D**) for the 139 strains with higher YFP/FSC ratio.

477 **Figure 3. tRNA methyltransferases and Elongator activate MBF.** (**A**) Plot of FITC
478 (YFP fluorescence) vs FSC corresponding to the 2792 strains of the knock-out
479 collection with the values of the knock-out strains of genes involved in tRNA
480 methylation highlighted in red. (**B**) Total RNA from wild type (WT), Δ*yox1*, Δ*rep2*,
481 *Δtrm112*, *Δmtq2*, *Δtrm9*, *Δtrm11,* Δlys9 and Δ*bud23* strains was analyzed by Northern
482 blot. Hybridization with an actin (*act1*) probe and the staining of rRNA is shown as
483 loading control. FI: Signal was quantitated and normalized relative to the signal of the
484 wild type strain. (**C**) Spot assay of the same strains by serial dilution and growth in rich
485 media or in media with 5 mM HU. Plates were incubated at 30ºC for 3-4 days. (**D**)
486 TCA extracts from wild type (WT) and *Δtrm112* strains expressing Rep2-HA were
487 immunoblotted with α-HA to detect Rep2. Ponceau staining is shown as loading

488 control. (**E**) Same as in (A), highlighting knock-out strains of Elongator. (**F**) Total
489 RNA from wild type (WT), Δ*yox1*, Δ*rep2*, Δiki3 and Δ*ctu1* strains was analyzed by
490 Northern blot. *act1* hybridization and *rRNA* are shown as loading controls. FI: Signal
491 was quantitated and normalized relative to the signal of the wild type strain.

492 **Figure 4. COP9/Signalosome down-regulates MBF-dependent transcription.** (**A**)
493 Plot of FITC (YFP fluorescence) vs FSC corresponding to the 2792 strains of the
494 knock-out collection with the knock-out strains of COP9/signalosome highlighted in
495 red. (**B**) Total RNA from cultures of wild type (WT), Δ*yox1*, Δ*rep2*, *Δcsn1*, *Δcsn2*,
496 *Δddb1*, *Δcdt2* and Δ*spd1* strains was analyzed by Northern blot by hybridization with
497 the *cdc18* probe. *rRNA* and *act1* are shown as loading controls. FI: Signal was
498 quantitated and normalized relative to the signal of the wild type strain. (**C**) Yox1
499 phosphorylation is detected in the strains indicated on top. Wild type (WT) and wild
500 type treated with HU (WT + HU) are shown as phosphorylation control. (**D**) Spot assay
501 of the same strains (plus Δ*spd1*Δ*ddb1* and Δ*spd1*Δcdt2) analyzed by serial dilution and
502 growth in rich media or in media with 5 mM HU. Plates were incubated at 30ºC for 3-4
503 days. (**E**) Tetrad dissection of *Δddb1 c*rossed with *Δrad3* strains. (**F**) Tetrad dissection
504 of *Δddb1 c*rossed with *Δcds1* strains.

505

Table 1. Strains with down-regulated MBF activity

Systematic name	Gene name	FITC/FSC ratio
SPBC36.07	elp1	0.52
SPCC11E10.06c	elp4	0.52
SPAC30.02c	kti2	0.53
SPAC26A3.07c	rpl1101	0.54
SPBC2F12.11c	rep2	0.55
SPAC1071.02	mms19	0.55
SPAC25G10.06	rps2801	0.55
SPAPB17E12.05	rpl3703	0.55
SPAC10F6.13c		0.55
SPBC3H7.07c	ser2	0.56
SPBC3H7.10	elp6	0.58
SPAPB1E7.06c	eme1	0.58
SPAC31A2.02	trm112	0.58
SPAC323.05c		0.59
SPAC12G12.13c	cid14	0.59
SPAC1250.03	ubc14	0.60
SPCC74.05	rpl2702	0.60

506

Table 2. Strains with up-regulated MBF activity

Systematic name	Gene name	FITC/FSC ratio
SPBC16A3.07c	nrm1	5.39
SPBC21B10.13c	yox1	4.91
SPAC17H9.10c	ddb1	2.90
SPAC17A5.14	exo2	2.56
SPBC215.03c	csn1	2.49
SPAPB17E12.04c	csn2	2.37
SPAC23C4.11	atp18	2.09
SPBC3E7.15c	mug83	2.02
SPCC338.16	pof3	1.94
SPAC22F3.09c	res2	1.94
SPAC17H9.19c	cdt2	1.94
SPBC365.14c	uge1	1.92
SPBC19G7.10c	pdc2	1.91
SPBC31E1.02c	pmr1	1.84
SPBC16G5.15c	fkh2	1.83
SPAPB1A10.15	arv1	1.79
SPBC30B4.04c	sol1	1.79
SPBC106.20	exo70	1.76
SPAC30D11.10	rad22	1.68
SPAC6G10.06		1.68
SPCC126.04c	sgf73	1.64
SPCC18.01c	adg3	1.63
SPAC14C4.09	agn1	1.61
SPBC19G7.06	mbx1	1.61
SPBC354.12	gpd3	1.57
SPAC16E8.01	shd1	1.57
SPBC337.03	rhn1	1.56
SPBC19C7.12c	omh1	1.56
SPAC4F10.13c	mpd2	1.56
SPAC694.06c	mrc1	1.56
SPBC24C6.10c	dip1	1.55
SPCC162.11c		1.55

507

Table 3. Strains used in this study

Strain	Genotype	Origin
972	*h-*	Lab stock
JA0801	*yox1-13Myc-NatR+ ura4-D18 h-*	(11)
JA0993	*rad3::NatR+ h-*	This work
JA1159	*cds1::NatR+ h-*	Lab stock
JA1512	*rep2::KanR+ h-*	This work
JA1818	*cdc22-YFP-Hyg pSty1-HA-mRFP (int @ leu1) leu1::natMX6 leu1-32 h+*	This work
JA1845	*cdc22-YFP-Hyg pSty1-HA-mRFP (int @ leu1) leu1::natMX6 mat1_m-cyhS, smt0; rpl42::cyhR (sP56Q) leu1-32 h-*	This work
JA1879	*yox1::NatR+ h+*	This work
JA1935	*csn1::KanMX4 h+*	This work
JA1936	*csn2::KanMX4 h-*	This work
JA1994	*csn1::KanR+ yox1-13Myc-NatR+ h+*	This work
JA1996	*cdt2::KanMX4 h-*	This work
JA2008	*ddb1::KanMX4 h+*	This work
JA2009	*spd1::KanMX4 h-*	This work
JA2011	*ddb1:KanR+ yox1-13Myc-NatR+ ura4-D18 h-*	This work
JA2012	*cdt2:KanR+ yox1-13Myc-NatR+ ura4-D18 h+*	This work
JA2028	*spd1::KanMX4 cdt2::KanMX4 yox1-13Myc-NatR+ h-*	This work
JA2083	*csn2::KanR+ yox1-13xMyc-NatR+ h-*	This work
JA2092	*spd1::KanR+ yox1-13xMyc-NatR+ h+*	This work
JA2094	*ddb1:KanR+ yox1-13Myc-NatR+ spd1::KanR+ ura4-D18 h+*	This work
JA2103	*rep2:3xHA-NatR+ h-*	This work
JA2142	*rep2:3xHA-NatR+ trm112::KanR+ h-*	This work
JE23	*mtq2::KanR+ h-*	This work
JE24	*lys9::KanR+ h+*	This work
JE25	*trm9::KanR+ h-*	This work
JE33	*trm11::KanR+ h-*	This work
JE34	*trm112::KanR+ h+*	This work
P392	*ade6-M210 leu1-32 ura4-D18 mat1_m-cyhS smt0 rpl42::cyhR (sP56Q) h-*	(27)
PG141	*bud23::KanR+ h-*	This work

508

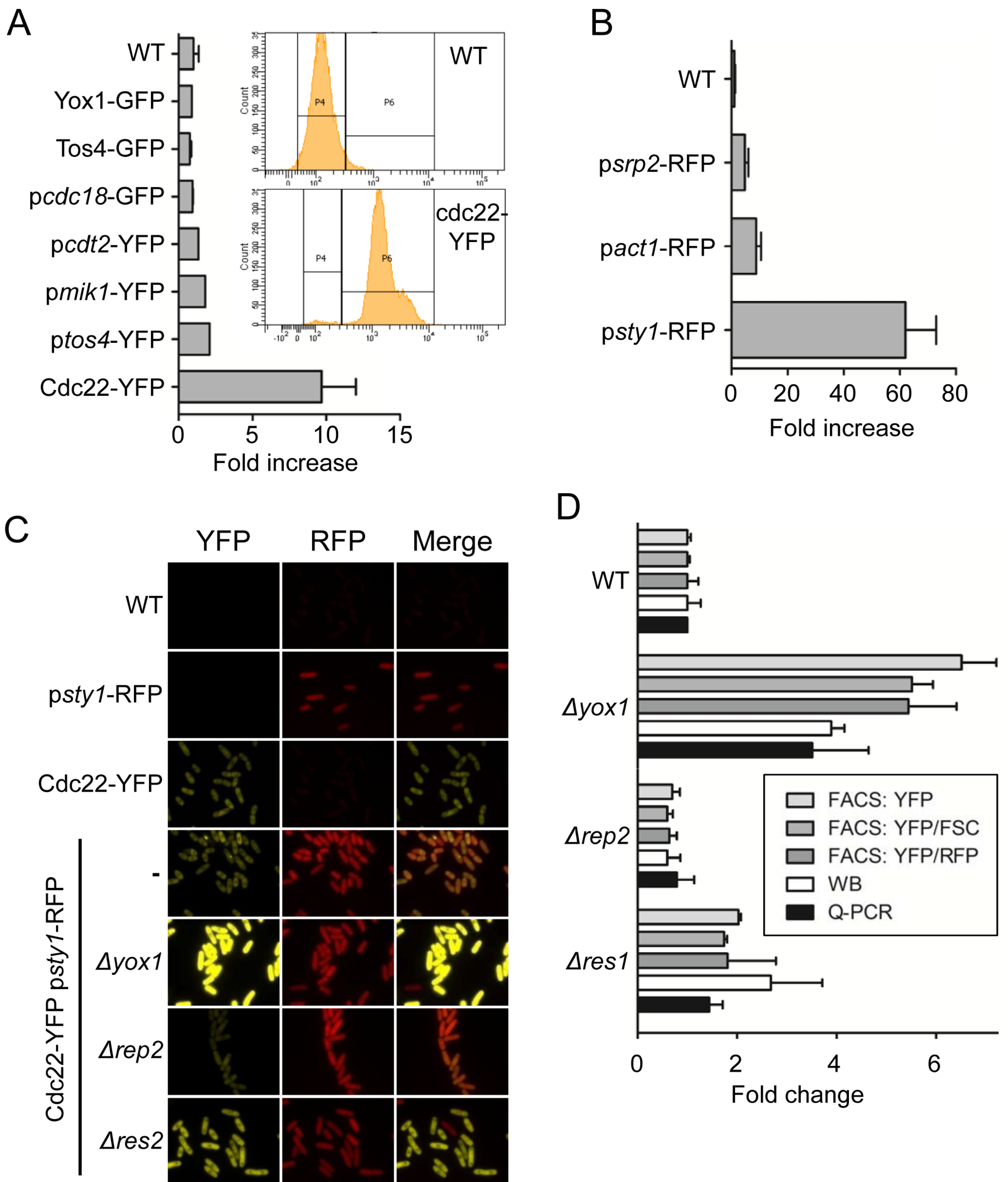

Gaspa et al.
Figure 1

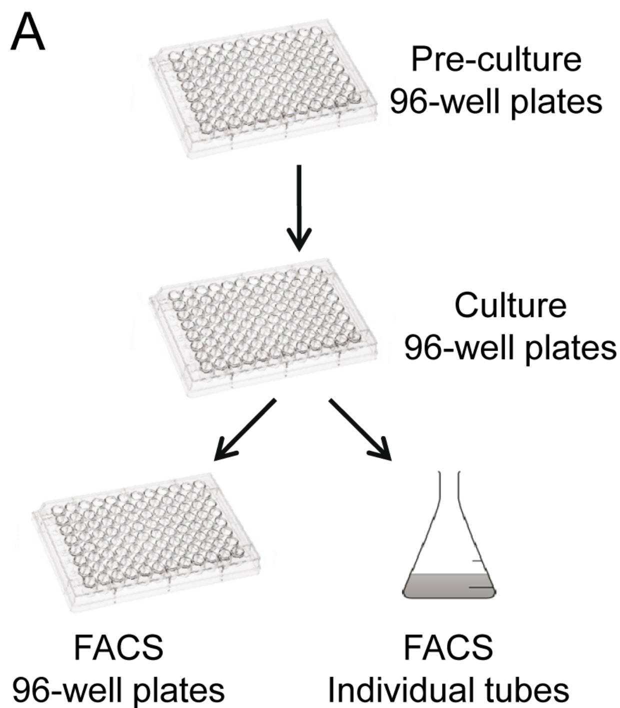

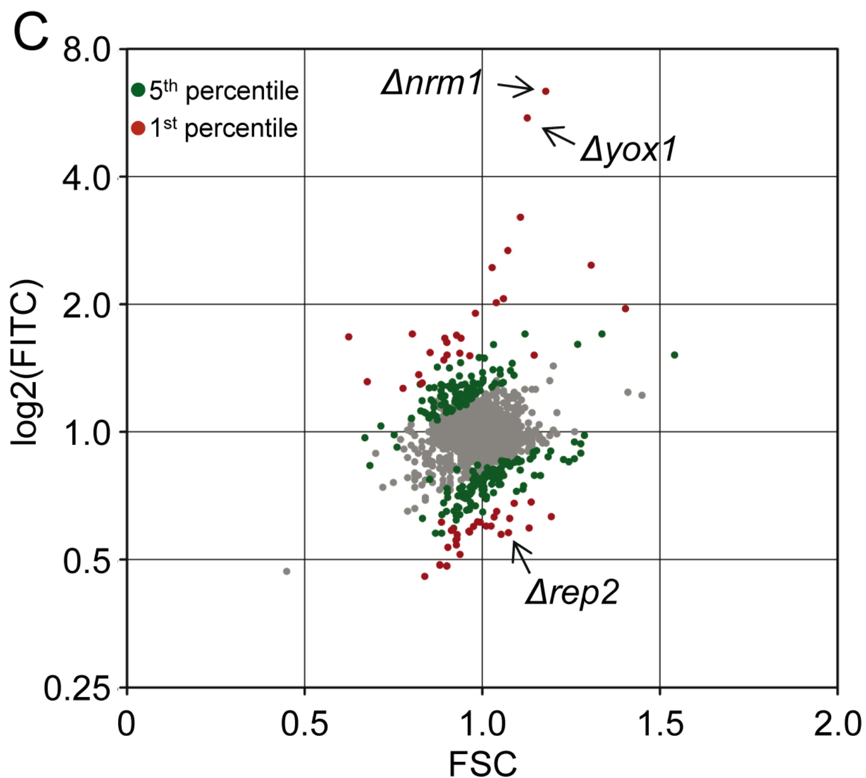

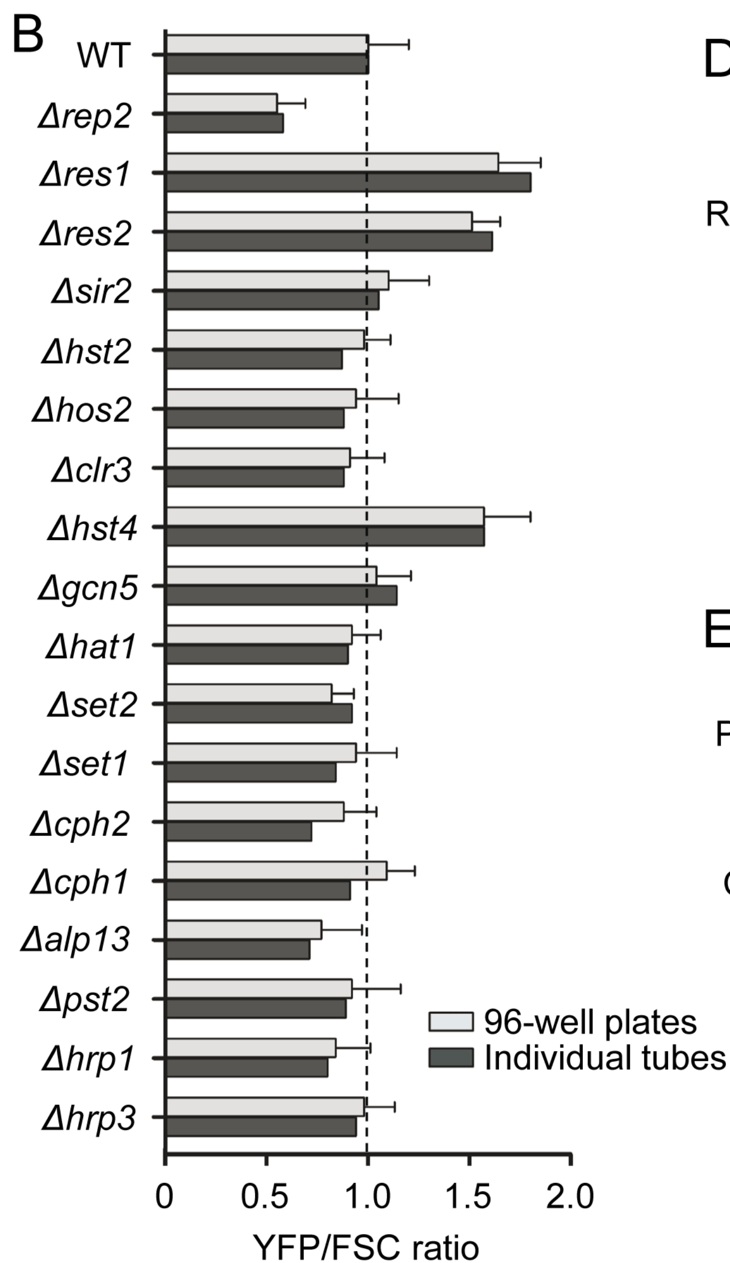

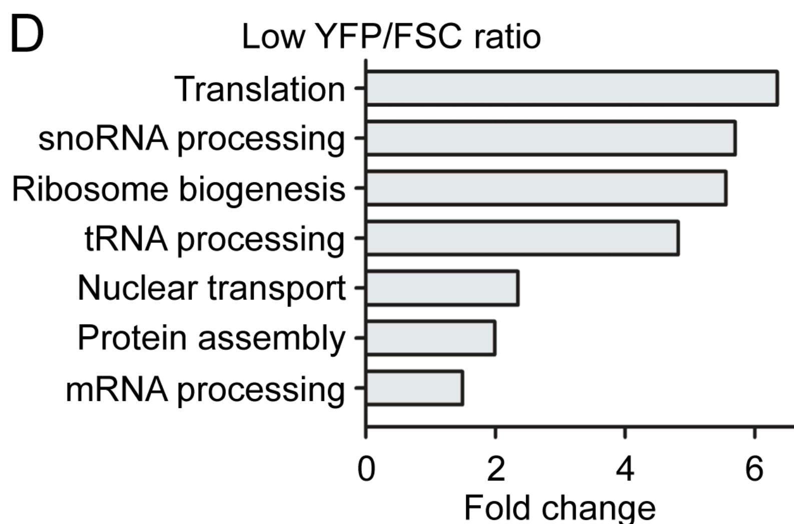

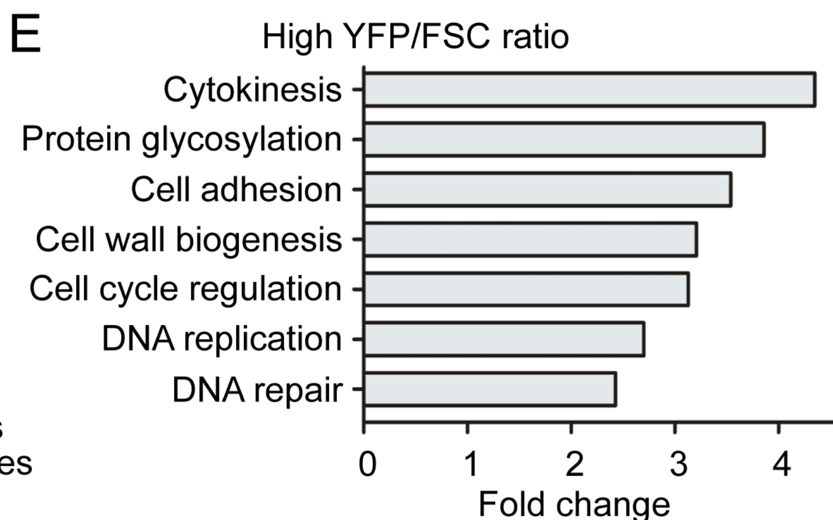

Gaspa et al.
Figure 2

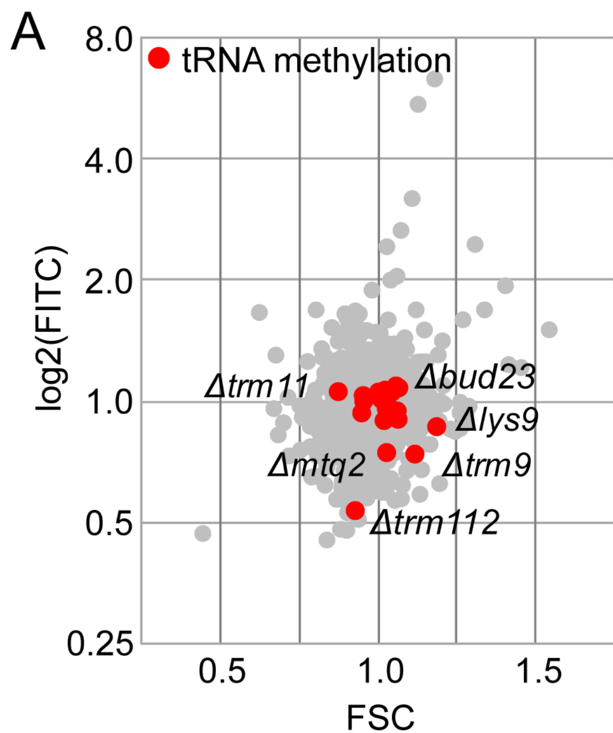

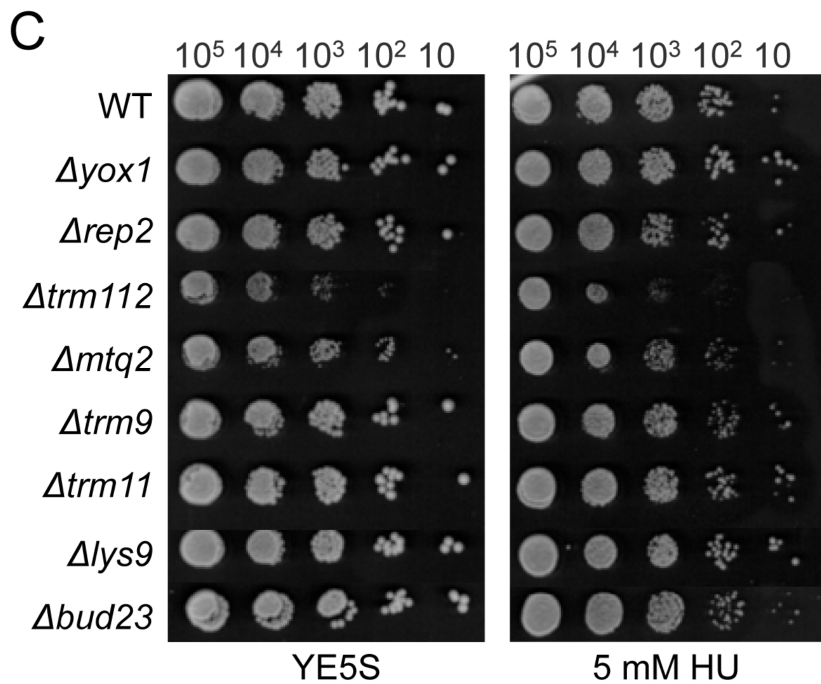

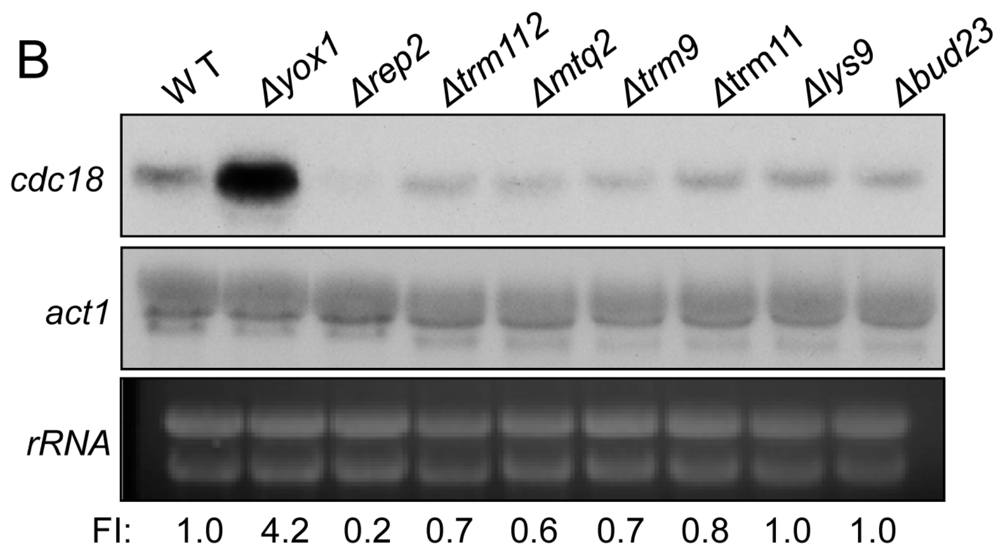

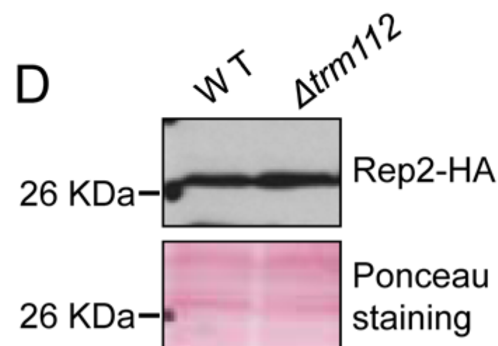

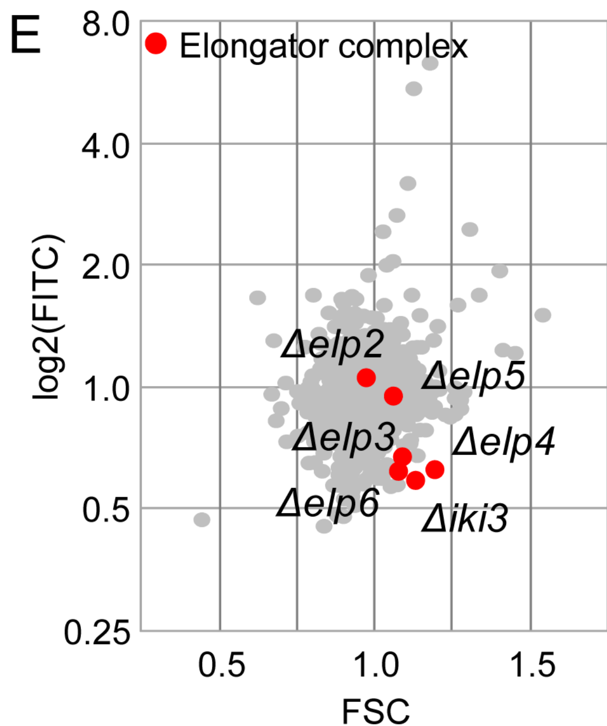

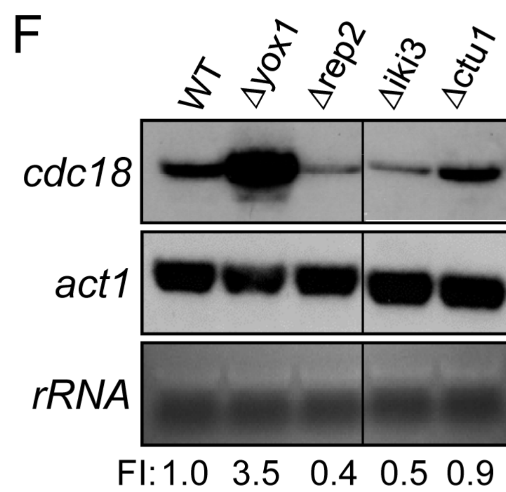

Gaspa et al.
Figure 3

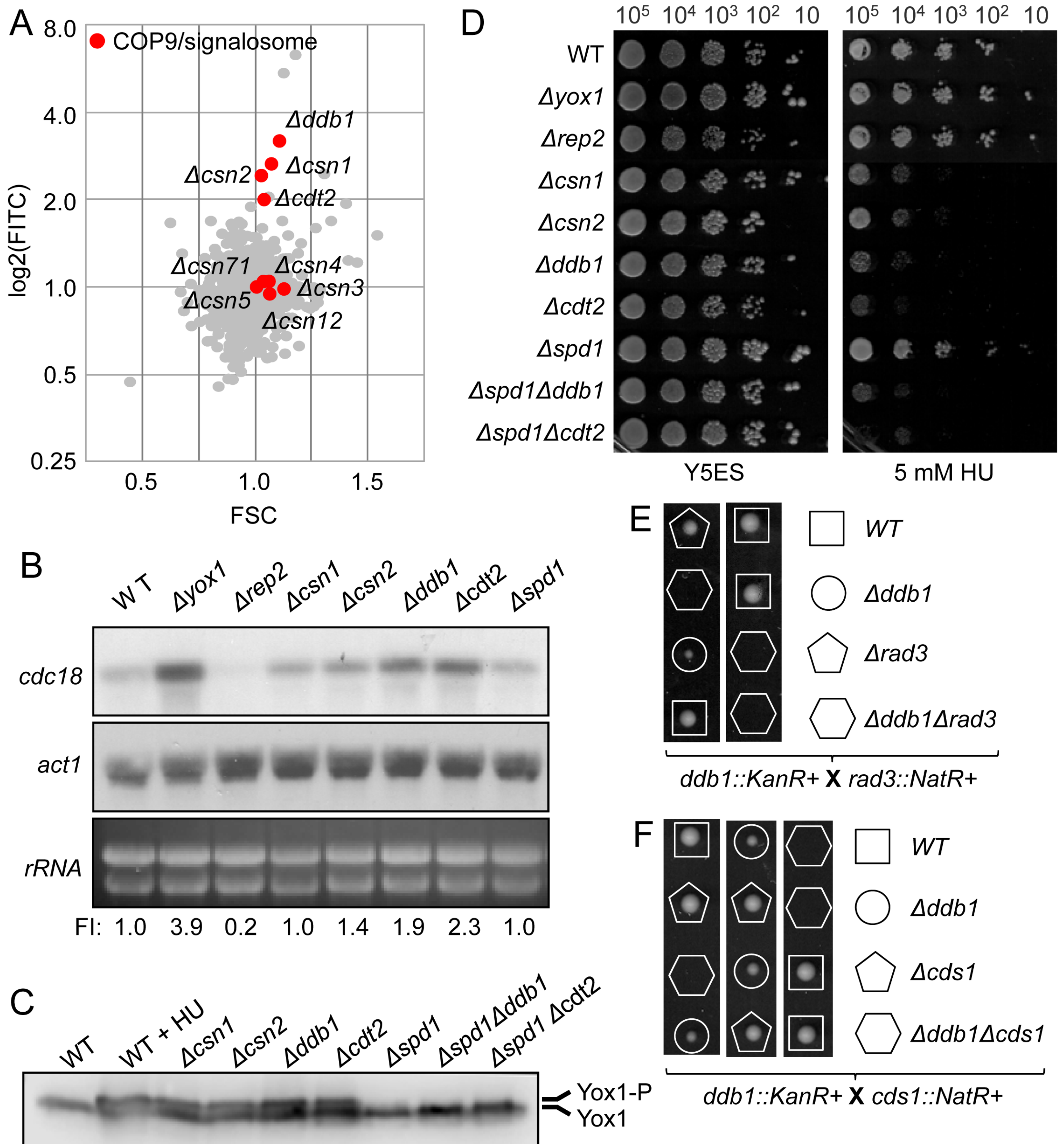

Gaspa et al.
Figure 4